

This discussion paper is/has been under review for the journal *Atmospheric Chemistry and Physics (ACP)*. Please refer to the corresponding final paper in *ACP* if available.

**Linking aerosol
fluxes in street
canyons to urban
city-scale emissions**

B. K. Tay et al.

Linking aerosol fluxes in street canyons to urban city-scale emissions

**B. K. Tay¹, G. B. McFiggans¹, D. P. Jones², M. W. Gallagher¹, C. Martin¹,
P. Watkins², and R. M. Harrison³**

¹Centre for Atmospheric Science, SEAES, The University of Manchester, Manchester, M13 9PL, UK

²School of Mechanical, Aerospace and Civil Engineering, The University of Manchester, P.O. Box 88, Manchester M60 1QD, UK

³Division of Environmental Health and Risk Management, School of Geography, Earth and Environmental Sciences, University of Birmingham, Edgbaston, Birmingham B15 2TT, UK

Received: 12 August 2009 – Accepted: 17 August 2009 – Published: 1 September 2009

Correspondence to: M. W. Gallagher (martin.gallagher@manchester.ac.uk)

Published by Copernicus Publications on behalf of the European Geosciences Union.

Title Page

Abstract

Introduction

Conclusions

References

Tables

Figures



Back

Close

Full Screen / Esc

Printer-friendly Version

Interactive Discussion

Abstract

In this study we investigate ultrafine particle (UFP) fluxes using a first order eddy viscosity turbulence closure Computational Fluid Dynamics (CFD) model and determine the different factors that influence emissions of UFP into the urban boundary layer.

Both vertical turbulent fluxes as well as the fluxes due to mean flow are shown to contribute to the overall ventilation characteristics of street canyons. We then derive a simple parameterised numerical prediction model for canyon top UFP venting which is then compared with tower based micrometeorological flux measurements obtained during the REPARTEE and CityFlux field experiments.

1 Introduction

The spatial heterogeneity of urban street canyons and the complex interplay of chemically, spatially and temporally varying ultrafine particle (UFP) emission sources as a function of micrometeorological and meteorological factors represents a challenge to both computational fluid dynamical modelling approaches and field observations.

Approaches adopting intensive measurement campaigns or networks generally have either insufficient spatial resolution, temporal or compositional and size spectral resolution to represent aerosol adequately. Experimental approaches however must be informed by appropriate numerical dispersion modelling combined with realistic aerosol physico-chemical descriptions to be of benefit when interpreting and applying measurements to exposure and epidemiological studies. Predictions of the vertical and horizontal structure of aerosol concentrations in street canyons are therefore required to inform future directives regarding recommended sampling and monitoring protocols.

In this study we investigate ultrafine particle (UFP) fluxes using a first order eddy viscosity turbulence closure Computational Fluid Dynamics (CFD) model and determine the different factors that influence the UFP fluxes into the urban boundary layer. Both vertical turbulent fluxes as well as the fluxes due to mean flow are shown to contribute

Linking aerosol fluxes in street canyons to urban city-scale emissions

B. K. Tay et al.

Title Page

Abstract

Introduction

Conclusions

References

Tables

Figures



Back

Close

Full Screen / Esc

Printer-friendly Version

Interactive Discussion

to the overall ventilation characteristics of a street canyon. We then derive a simple parameterised numerical prediction model for canyon top UFP venting. The simple model is then compared with tower based micrometeorological flux measurements reported in recently published field studies including the REPARTEE and CityFlux experiments.

5 Whilst undoubtedly crude these comparisons may be used as a starting point for linking street level parameters to those measured above the urban roughness layer with potential for validating high resolution city-scale air quality models.

2 Background

10 Understanding ventilation characteristics from built environments via idealised canyon structures under a range of canyon flow conditions is an aid to predicting average UFP pollutant concentrations within these structures for street level pollutant exposure assessment and pollutant monitoring network designs and interpretation of their data. It is also the first step in coupling street level aerosol concentrations to net city scale emission fluxes measured above the urban roughness layer, for regional and climate model impact and mitigation studies.

15 Implicit in most operational street canyon models is that the canyon is venting vertically. Whilst it is understood that fluxes from street canyons are governed by both turbulent and advective processes, the relative importance and contribution of each process is a topic of ongoing research. Advection originates from roof level wind conditions. The sources of turbulence contributing to this venting are buoyancy, turbulent shear at the surfaces, traffic movement and the turbulent intensity (Ti , *the ratio of the root-mean-square of the velocity fluctuations, u' , to the mean flow velocity*) of the canyon inflow. If we consider the case of wind blowing perpendicular to a canyon axis, the layer of strong shear that develops at the canyon top is believed to oscillate, driving an intermittent mixing circulation around the street canyon (De Paul, 1986; Belcher, 2005) and hence the vertical flux from the canyon. Using a simple 2-D CFD model coupled with the $k-\varepsilon$ turbulence model and considering wind perpendicular to the longitudinal

Linking aerosol fluxes in street canyons to urban city-scale emissions

B. K. Tay et al.

Title Page

Abstract

Introduction

Conclusions

References

Tables

Figures

⏪

⏩

◀

▶

Back

Close

Full Screen / Esc

Printer-friendly Version

Interactive Discussion

**Linking aerosol
fluxes in street
canyons to urban
city-scale emissions**

B. K. Tay et al.

Title Page

Abstract

Introduction

Conclusions

References

Tables

Figures

⏪

⏩

◀

▶

Back

Close

Full Screen / Esc

Printer-friendly Version

Interactive Discussion

axis of an idealised canyon, (e.g. *aspect ratio* $AR=H/W \sim 0.5-2$ where H is the canyon height and W its width; *Turbulent Intensity* $\sim 0.001-0.025$ and wind speeds ≤ 5 m/s) it can be shown that the turbulent flux contribution dominates the net vertical flux of pollutants compared to the advective flux. The net effect of turbulent flux therefore is to exhaust pollutants whilst the net effect of advective flux is to re-entrain aerosols (Baik, 2002). Using Large Eddy Simulation approaches it has been found that this removal process takes place over relatively long timescales. Pollutants intermittently travelling up the leeward face of a canyon require sufficient momentum to penetrate the shear layer present at canyon top-boundary layer interface and be transported into the overlying boundary layer. The timescales for these processes is $\sim 30-60$ s and it is the larger scale eddies that are responsible for the removal of the majority of pollutants instead of small scale turbulence (Walton, 2002).

There is evidence from past experimental studies that canyon ventilation is a function of a range of flow conditions, in particular turbulence, wind speed and canyon geometry. In a field study, DePaul and Sheih (1985) found that the ventilation velocity of a tracer from a canyon with aspect ratio $AR=1.5$ was correlated with both friction velocity, u_* , at the roof level, and the horizontal wind, U . In addition, Barlow (2002) found that the street canyon aspect ratio is an important factor in influencing the ventilation efficiency. She found that amongst all flow regimes, ventilation efficiency was dominant for wake-interference flow. Both studies found a robust relationship between ventilation velocity, v_H , and horizontal wind component, U_H . Barlow (2002) further suggested that this implied the scalar transport was controlled by turbulence. This hypothesis is consistent with the numerical studies referred to above.

In spite of extensive studies on the escape of pollutants from street canyons, there are still several research questions warranting further investigation. There has been little attempt to parameterise flux from street canyons at a range of turbulent intensities and wind speeds and for different canyon aspect ratios. The coupling of surface fluxes and dynamics to city scale fluxes for large-scale models, within the urban canopy, though plausible, has also received little attention. Finally, whilst the dominance of tur-

bulent flux under isothermal conditions, where only forced convection is taking place, has been demonstrated, the influence of thermal effects (natural convection) on the relative extents of both turbulent and advective fluxes has not been studied in detail. The influence of both natural and forced convection on the different components of aerosol fluxes needs further investigation.

3 Model framework

For this study a 2-D Computational Fluid Dynamics (CFD) modelling platform based on the incompressible finite volume method was used. The mass, momentum and standard $k-\varepsilon$ turbulence model equations representing the continuous phase were solved. An additional energy equation was solved when considering buoyancy cases based on the Boussinesq Approximation. The discrete phase, representing UFP, was characterised via the Euler-Euler multiphase approach (Whitby, 1991) and assumed to be transported by the velocity field for the continuous phase. The equations were solved using the deferred correction Total Variation Differencing Scheme except for the turbulence equations, which were solved using the Upward Differencing Scheme. The SIMPLE (Semi Implicit Method for Pressure Linked Equations) pressure-velocity coupling scheme was used to obtain the velocity field. Details may be found in Ferziger and Peric (1999) and Versteeg and Malalasekera (2007). Steady-state solutions were obtained for all cases. The code was validated against reference wind tunnel dispersion data, Ketzler et al. (2000, Trapos network) and good comparisons were obtained.

The computational domain comprised a symmetrical inlet (velocity inlet) and outlet with a cavity below representing the idealized street canyon. Smooth wall boundary conditions were used. The vertical and horizontal inlet scales were 5 and 2× the vertical cavity dimension, and the outlet horizontal scale was 10× the cavity dimension. The height of the canyon was chosen to be 10 m, a typical length scale expected in urban environments. Boundary conditions were located at a distance such that they would not interfere with the numerical results within the cavity. A structured mesh was used.

Linking aerosol fluxes in street canyons to urban city-scale emissions

B. K. Tay et al.

Title Page

Abstract

Introduction

Conclusions

References

Tables

Figures



Back

Close

Full Screen / Esc

Printer-friendly Version

Interactive Discussion



The domain had a total of e.g. 70, 500 grid cells for a typical 10 m by 10 m canyon. Appropriate values representing a range of meteorological conditions were used at the inlet boundary conditions where a uniform wind speed profile (U) was imposed representing wind blowing perpendicular to the canyon axis. The range of wind speeds selected represented the flow regime where the extent of forced convection was such that vehicular turbulence could be ignored (Kumar et al., 2009). The turbulent kinetic energy profile at the inlet boundary condition was set equal to:

$$k = 1.5 \times Tl \times U^2 \quad (1)$$

and the inlet turbulent dissipation profile was set to:

$$\varepsilon = C_{\mu}^{0.75} k^{1.5} \kappa^{-1} z^{-1} \quad (2)$$

with $C_{\mu}=0.09$ and $\kappa=0.4$. The dissipation length scale (z) was taken to be 0.07 of the characteristic length scale of the velocity inlet (Versteeg and Malalasekera, 2007).

To represent vehicle exhaust plumes, an elevated finite cross sectional line “emission source” 0.3 m above ground was imposed with a predetermined concentration level of the discrete phase. The aerosol characteristics (Table 1) were chosen based on an a-priori assumption of a typical UFP (Aitken) and accumulation aerosol lognormal size distribution for representative concentrations 1 m from a vehicle exhaust pipe. The dilute nature of UFP is consistent with the one-way coupling assumption. The turbulent Schmidt number was set to 1, assuming turbulent diffusion of the discrete phase occurred to the same extent as the turbulent diffusion of momentum.

Examples of flow fields for isothermal cases are shown in Fig. 1a–c for canyon aspect ratios AR=0.5, 1.0 and 2.0, respectively whilst Fig. 2a–c are for mixed convection cases for; a leeward heated wall canyon; windward heated wall canyon; and a windward heated wall canyon for transitional flow, respectively. These will be referred to in more detail below.

Linking aerosol fluxes in street canyons to urban city-scale emissions

B. K. Tay et al.

Title Page

Abstract

Introduction

Conclusions

References

Tables

Figures

⏪

⏩

◀

▶

Back

Close

Full Screen / Esc

Printer-friendly Version

Interactive Discussion

3.1 Characterisation of turbulent and advective aerosol flux components

In this study both turbulent and advective fluxes were evaluated through the interface of the canyon top and free flow regime above. The components of the net advective flux investigated in this case are the updraft and downdraft contributions at the leeward and windward side of the canyon, respectively which are compared to the turbulent aerosol fluxes which originate from the Reynolds stresses of aerosol concentration arising from unsteady, turbulent flows. A positive flux implies a net venting from the canyon while negative flux implies a net re-entry into the canyon. The vertical UFP flux due to mean flow is, $F_a = \bar{w} \bar{\chi}$; where $\bar{\chi}$ is the mean UFP concentration and \bar{w} is the mean vertical velocity at canyon top level. The vertical flux of UFP due to turbulent flows is: $F_a = \overline{w' \chi'} = -K_\chi \frac{\partial \bar{\chi}}{\partial z}$ where χ' is the deviation from the mean concentration and w' is the deviation from the mean vertical velocity and z is height. Implementing a first order eddy viscosity turbulence closure model, turbulent flux may be characterised as the product of K_χ , the turbulent diffusivity (eddy viscosity) of the aerosol, and the vertical gradient of aerosol concentration. Integration of the flux across the horizontal direction yields the net flux due to advective flow, $F_a = \int_L F_a dx$, and turbulent flow $F_t = \int_L F_t dx$, where L is the canyon dimension. The net flux from both processes along the horizontal axis of the canyon at roof level is thus expressed as:

$$F_{\text{Net}} = \int_L \left(-K_\chi \frac{\partial \bar{\chi}}{\partial z} + \bar{\chi} \bar{w} \right) dx. \quad (3)$$

3.1.1 Isothermal cases

A series of 9 cases for 3 different canyon aspect ratios were simulated using 3 wind speed and 3 turbulence regimes in each case. Natural buoyancy effects due to heated walls and exhaust plumes are ignored in these cases. The Reynolds Number $Re = \frac{U \rho H}{\mu}$ (where ρ is the air density, μ the viscosity, and U , the canyon inflow wind speed measured at a reference height, and H is again the canyon height) is the ratio of the inertial

Linking aerosol fluxes in street canyons to urban city-scale emissions

B. K. Tay et al.

Title Page

Abstract

Introduction

Conclusions

References

Tables

Figures

◀

▶

◀

▶

Back

Close

Full Screen / Esc

Printer-friendly Version

Interactive Discussion



and viscous forces. Re was found to range from 1.7×10^6 to 6.7×10^6 . Table 2 summarises the parameter space for the studies where Tl and inflow levels are referred to hereafter as low, medium and high cases.

3.1.2 Mixed convection cases

To investigate the influence of thermal effects within canyons on the aerosol flux, a canyon of unity aspect ratio was considered and the temperature of the aerosol source exhaust was assumed to be 300 K, whilst air temperature above the canopy was 290 K. The highest Tl value was assumed for these cases. The leeward and windward walls of the canyon were heated to different extents to represent different levels of contribution to mixed convection. The relative thermal effects of buoyancy and forced convection within a street canyon may be determined based on the Richardson Number, $Ri = \frac{gH\Delta T}{U^2 T_0}$, the ratio of potential to kinetic energy where g is the gravitational constant, ΔT is the temperature difference between the heated wall and the above canyon flow, and T_0 is the above-canyon air temperature. At low Ri , the temperature difference between the heated wall and the fluid is small and the wind speed large enough so that buoyancy effects may be ignored, but beyond a critical value, buoyancy becomes important enough to affect the overall fluid flow pattern. Table 3a–c summarises the ranges of parameter space tested.

3.2 Model results

3.2.1 Isothermal cases

Skimming flow was observed for all cases considered, characterized by a main clockwise vortex extending throughout the canyon geometry and 3 minor anti-clockwise vortices at the two corners of the leeward side as well as the bottom corner of the windward side, Fig. 1a. Compared with other geometries ($AR=0.5$ and 2.0), the corner vortices are more dominant at $AR=1.0$. The centre of the vortex appeared in the

Linking aerosol fluxes in street canyons to urban city-scale emissions

B. K. Tay et al.

Title Page

Abstract

Introduction

Conclusions

References

Tables

Figures

⏪

⏩

◀

▶

Back

Close

Full Screen / Esc

Printer-friendly Version

Interactive Discussion



Linking aerosol fluxes in street canyons to urban city-scale emissions

B. K. Tay et al.

[Title Page](#)[Abstract](#)[Introduction](#)[Conclusions](#)[References](#)[Tables](#)[Figures](#)[⏪](#)[⏩](#)[◀](#)[▶](#)[Back](#)[Close](#)[Full Screen / Esc](#)[Printer-friendly Version](#)[Interactive Discussion](#)

middle of the canyon when the aspect ratio (H/W) was 1.0 and 2.0, displacing to the windward side when the aspect ratio was 0.5, Fig. 1c. This agrees with Johnson and Hunter's (1999) observations of a skimming flow regime down to an aspect ratio of 0.4 (below which wake-interference flow takes over) and Solazzo's (2007) numerical simulations, assuming smooth wall boundary conditions. This contrasts with other studies where a dual-vortex skimming flow regime was observed at $AR \sim 2.0$ when rough wall conditions were considered, with a transitional threshold to the wake-interference flow observed at $AR = 0.65$, (e.g. Hunter et al., 1992; Sini et al., 1996). Figure 2 shows an example of flow streamlines produced with a mixed convection case for a canyon with $AR = 1.0$ (leeward canyon wall heated, low wind speed $U = 2.5$ m/s and temperature difference $\Delta T = 4$ K). Figure 2b shows an example of flow streamlines produced with a mixed convection case for a canyon with $AR = 1.0$ (windward canyon wall heated, low wind speed $U = 2.5$ m/s and temperature difference $T = 4$ K) and Fig. 2c shows a dual vortex flow when ΔT is increased to 15 K. This flow regime transition takes place when $\Delta T = 10$ K at $U = 2.5$ m/s. These results are analysed in detail below.

3.2.2 Concentration profiles

Before discussing in detail the results for aerosol fluxes we note in passing that some CFD experiments have shown varying degrees of success in representing real-world UFP concentration profiles measured in street canyons. Figure 3a is the leeward canyon vertical UFP concentration profile predicted using this model for low and high wind speed (skimming-perpendicular flow) cases ($U = 2.5$ and 10 m/s) and low, medium and high Tl cases. The predicted profile structure can be split into three general layers; a layer near street level where concentrations increase rapidly to a maximum value, a middle layer where the concentration follows an approximate exponential decrease and a turbulent shear layer at the top of the canyon where the concentration declines more rapidly. The predicted leeward profile appears to be in reasonably qualitative agreement with the field measurements of Kumar et al. (2009), also shown in Fig. 3, despite the simplifications, although such measurements are sparse. Figure 3b also

compares this with the windward concentration profile that has different characteristics which need to be considered in the design and interpretation of canyon field experiments.

3.2.3 Aerosol fluxes

5 Consistent with Baik's (2002) studies, for all cases, F_{Net} was found to be positive, implying a net venting of aerosols into the urban boundary layer. The greater magnitude of flux at lower AR suggests that natural ventilation is poor in a street canyon with larger AR. The magnitude of turbulent flux, F_t , was higher than the advective flux, F_a , by at least an order of magnitude for all cases, consistent with the data reported by
10 Baik (2002), except for shallow canyons (AR=0.5) at 10 m/s when the turbulent flux is higher by 2 orders of magnitude. A positive F_t , (venting of aerosols), was observed for all AR. F_a was positive when AR=0.5 but negative (re-entrainment of aerosols) for the other geometries. When considering forced convection alone and when effects of buoyancy may be ignored, the turbulent flux dominates the ventilation process. This is
15 consistent with the suggestion of Barlow (2002).

For a given wind speed, an increase in Tl will result in a proportional increase in F_t . For all cases considered, there is an increase in F_t with increasing Tl as expected for a given U , Fig. 4. It was observed that the sensitivity of F_t to Tl is dependent on AR, being strongest for the symmetrical (AR=1.0) canyon. The reasons for the weaker
20 sensitivity for AR=0.5 and 2 are different. F_t is a function of eddy viscosity, μ , and concentration shear, $d\chi/dz$. For all cases, the increase in Tl increases the mean μ . When Tl increases from ~ 0.05 to 0.1, the overall shear will increase (due to enhanced vertical advection) but, when Tl increases from ~ 0.1 to 0.26, the concentration gradient decreases due to the enhanced turbulent mixing of pollutants. These trends are
25 summarised in Fig. 5, for the case $U=10$ m/s, which shows the vertical concentration gradient ($d\chi/dz$) as a function of normalised distance, X/W (centre of canyon zero, lee-windward wall -1 and windward wall $+1$), across the canyon, and for the different canyon aspect ratios. Considering both the shallow and deep canyons, the maximum concen-

Linking aerosol fluxes in street canyons to urban city-scale emissions

B. K. Tay et al.

Title Page

Abstract

Introduction

Conclusions

References

Tables

Figures

⏪

⏩

◀

▶

Back

Close

Full Screen / Esc

Printer-friendly Version

Interactive Discussion



Linking aerosol fluxes in street canyons to urban city-scale emissionsB. K. Tay et al.

[Title Page](#)[Abstract](#)[Introduction](#)[Conclusions](#)[References](#)[Tables](#)[Figures](#)[◀](#)[▶](#)[◀](#)[▶](#)[Back](#)[Close](#)[Full Screen / Esc](#)[Printer-friendly Version](#)[Interactive Discussion](#)

tration shear occurs just next to the leeward side of the canyon, but for the symmetrical canyon, it is further away from the wall. For the deep canyon case, $H > W$, the decrease in concentration gradient was found to be less apparent and least sensitive to TI , taking place only at the windward side of the canyon. This implies minimal advection of turbulent quantities into deeper canyons and consequently the weakest sensitivity to TI . In contrast, however, considering the shallow canyon, $H < W$, enhanced mixing due to increased turbulence leads to a reduction of shear along the entire horizontal axis, which moderates the increase in F_t due to enhancement in eddy viscosity when TI increases. F_t for the $AR=1.0$ canyon, however, is the most sensitive to TI . This is because whilst there is a reduction in shear at the windward side of the canyon due to turbulent mixing, there is also a corresponding enhancement of shear at the leeward side in this case. This is not observed for the other two canyon geometries and therefore accounts for the greatest sensitivity.

3.2.4 Isothermal cases: turbulent and advective aerosol flux

For a given TI , an increase in U will result in a proportional increase in F_t , Fig. 6. This strong relation is consistent with observations by Barlow (2002) and DePaul (1986). This is because the increase in U enhances the eddy viscosity and concentration shear at the roof of the canyon.

Except for the shallow canyon case, the net effect of advection is to enhance entrainment of aerosols, Fig. 7. The positive net contribution by advective flux, F_a , in the shallow canyon case ($H < W$) occurs because the mean vertical velocity, W , is in the positive direction across the majority of the axis at roof level, due to the displaced vortex centre. For a given U , an increase in TI decreases the magnitude of F_a for $AR=1$ (F_a is negative). For $AR=0.5$, when F_a is positive for all cases, increases in TI will result in an increase in F_a . This means that the effect of enhanced turbulence for both canyon geometries is an increased loss of aerosols at the leeward canyon side. This trend is similar for both cases and reflects the strong interaction between in-canyon dynamics and the above-roof canopy flow for both canyon geometries resulting in venting-in at

the windward side and venting-out at the leeward side.

For canyon AR values=2.0 however, an increase in TI increases F_a (with increased entrainment). This reflects the weaker interaction between the canyon and the above-roof canopy flow, with one dominant advective direction at the windward side of the canyon. At all AR values for a given TI , the magnitude of F_a increases as the inflow U increases. This is because the vortex becomes more pronounced with increasing U .

3.2.5 Isothermal cases: net aerosol fluxes

The net flux, F_{Net} , obtained, from F_a and F_t , was then compared to both TI and U for AR=0.5, 1.0 and 2.0, respectively. An exponential relationship was observed between turbulence and F_N whilst the linear relationship between U and F_{Net} is characteristic of F_t , demonstrating the dominance of turbulence in the overall canyon venting process as expected. A multi-variable regression was performed, using *TableCurve 3DTM*, on the data to relate the mean flux from the canyon at roof level, F_{Net} , to different levels of TI and U . Several best-fit equations were proposed, and solutions with r^2 of at least 0.99 were considered. The simplest result, which seems to represent best boundary layer dynamical processes, took the following form;

$$F_{Net} = \exp(a + b \ln U + cTI) \quad (4)$$

where a , b and c are non-dimensional coefficients. This parameterisation applies for AR=0.5, 1 and 2, and in the skimming flow regime with a single canyon vortex. Table 4 summarises the coefficients obtained in each case. Coefficient b is similar for all aspect ratios, but a difference is observed for coefficient c , reflecting the different responses of flux to TI , discussed above. This parameterisation was derived for a range of U (2.5 to 10 m/s) and TI (5×10^{-2} – $0.26 \text{ m}^2/\text{s}^2$) for both an idealised smooth-walled canyon neglecting buoyancy, and, assuming only wind driven turbulence.

Title Page

Abstract

Introduction

Conclusions

References

Tables

Figures

⏪

⏩

◀

▶

Back

Close

Full Screen / Esc

Printer-friendly Version

Interactive Discussion

3.3 Mixed convection cases

It was found in the previous isothermal cases that the typical flow pattern was a main clockwise circulatory vortex with 3 minor vortices at the two corners of the leeward side as well as the bottom corner of the windward side. This is observed for all levels of Tl and U . Previous studies have shown that the direction of the vortex varies with solar angle (i.e. time of day) with respect to the canyon walls (Nakaruma and Oke, 1988). One explanation for this is mixed convection taking place within the canyon when canyon dispersion involves forced convection originating from roof level winds and natural convection from heated walls. This influence on the flow patterns as well as the increase in turbulence due to thermal effects would have implications for the net aerosol flux from canyons.

Here we discuss the effects of natural convection on the net aerosol flux. Two cases were considered: *leeward heated wall* and *windward heated wall* cases. A range of Ri were considered, in order to reflect the different extents of mixed convection and its implications for advective and turbulent aerosol flux components.

3.3.1 Mixed convection: leeward heated wall

When the leeward wall is heated, the air close to the wall moves upwards, reinforcing the existing main vortex, Fig. 2a. No change in flow regime is observed for all extents of mixed convection considered. Figure 8 summarise the influence of buoyancy on both F_a and F_t for $U=2.5$ m/s for increased heating of the leeward canyon wall (temperature difference ΔT) and Fig. 9 for cases $U=5$ and 10 m/s, respectively. For all cases, it was found that F_t was positive (net loss of aerosols) at the roof level of the canyon and relatively insensitive to ΔT . F_t is a function of the vertical aerosol concentration gradient and μ . Again looking at the variation along the horizontal canyon axis at roof level, for all cases the increase in temperature enhances the concentration gradient at the leeward side of the canyon. Although this should augment the turbulent flux, the steady state dispersion pattern of the eddy viscosity is such that the mean eddy

Linking aerosol fluxes in street canyons to urban city-scale emissions

B. K. Tay et al.

Title Page

Abstract

Introduction

Conclusions

References

Tables

Figures

⏪

⏩

◀

▶

Back

Close

Full Screen / Esc

Printer-friendly Version

Interactive Discussion

viscosity along the horizontal axis considered does not vary significantly. This explains the relative stability of turbulent flux across different extents of buoyancy.

In contrast, F_a is found to be a strong function of ΔT and a positive linear relationship is found for all extents of mixed convection. When forced convection is dominant the net effect of F_a is negative, with re-entrainment of aerosols. However, beyond a threshold level of natural convection (when $Ri > 0.1$), F_a is positive and would increase linearly, eventually reaching a similar order of magnitude as F_t when $Ri > \sim 0.43$. Net flux, F_{Net} shows a positive linear relation with increasing buoyancy, Fig. 10. However, the rate of increase in flux is dependent on the extent of forced convection and U , as shown in the figure. When the temperature difference is ~ 15 K, F_{Net} is greater at 2.5 m/s than at 5 m/s. This is due to the dominance of F_a due to natural convection at lower U . Normalising the increase in flux by the original isothermal flux, F_0 , we can attempt a relationship between the increase in flux with Ri , i.e.

$$\left(\frac{\Delta F_{Net}}{F_0}\right) = aRi = a\left(\frac{gH\Delta T}{U_{ref}^2 T_0}\right). \quad (5)$$

As expected a strong positive linear relationship ($r^2 = 0.99$) between Ri and the enhancement in aerosol flux, $(\Delta F/F)$, due to increasing buoyancy, was found which applies for symmetrical canyons and leeward heated walls with $0 < Ri < 0.81$, Fig. 11. This relationship is a first step towards a simple parameterisation of the aerosol flux with differing extents of mixed convection, but simple extension to other heated canyon patterns is not as straightforward.

3.3.2 Mixed convection: windward heated wall

When the windward wall surface temperature is greater than the air temperature, the air close to the surface is heated, creating an upward buoyancy flux that opposes the direction of bulk entrainment of air at the windward side. Due to the upward movement close to the heated wall, at steady state, the windward bottom vortex is enhanced, with one

Linking aerosol fluxes in street canyons to urban city-scale emissions

B. K. Tay et al.

Title Page

Abstract

Introduction

Conclusions

References

Tables

Figures

⏪

⏩

◀

▶

Back

Close

Full Screen / Esc

Printer-friendly Version

Interactive Discussion



main clockwise vortex (Fig. 2b). At higher buoyancy levels, a change in flow regimes from single-vortex skimming flow regime to a multi-vortex skimming flow regime was observed. As the transition occurs, the upward movement close to the heated wall splits the main clockwise vortex into two, Fig. 2b, reducing the extent of the upper leeward vortex. It was found that when $Ri=0.54$, a change in flow regime occurs. The implications for the net aerosol flux and the relative contributions of both advective and turbulent aerosol fluxes at various extents of mixed convection would need further investigation.

3.3.3 Windward heated wall: single-vortex skimming flow regime

Considering only the single vortex skimming flow regime, it was found that the contribution by F_t is positive (net loss of aerosols) at the roof level of the canyon for all cases, whilst that for F_a is negative. It was also observed that both flux components are relatively insensitive to the temperature difference, although they gently decrease in magnitude with increasing temperature (in spite of the increase in mean eddy viscosity), as there is an overall decrease in concentration shear along the horizontal axis at roof level.

Unlike the leeward case, F_a is relatively stable at the range of mixed convection considered (deviating by no more than 10%). This is because the main vortex and upper leeward minor vortex is maintained. The enhancement of the lower windward vortex has a minimal impact on F_{Net} . As the main vortex is maintained with no change in the location of its centre, the decrease in W at the windward side is balanced by an increased W at the leeward side. Therefore, the effect on F_{Net} is not as evident, unlike the leeward wall heated case. As F_a is typically an order of magnitude lower than F_t , the escape of aerosols is driven mainly by turbulent flux. This implies that the influence on the aerosol flux would not be a directly linear function with respect to Ri as was observed for the leeward heated wall case. The decrease is also smaller when compared with the leeward heated case (<10% decrease for Ri up to 0.20), as illustrated in Fig. 11.

Linking aerosol fluxes in street canyons to urban city-scale emissions

B. K. Tay et al.

Title Page

Abstract

Introduction

Conclusions

References

Tables

Figures

⏪

⏩

◀

▶

Back

Close

Full Screen / Esc

Printer-friendly Version

Interactive Discussion



3.3.4 Windward heated wall: dual-vortex skimming flow regime

Considering the case for $U=2.5$ m/s, we observed a transition from a single vortex flow (at $Ri\sim 0.21$) to a dual-vortex flow regime (at $Ri\sim 0.54$). In spite of the transition, the direction of turbulent and advective aerosol fluxes remains the same. This transition leads to a decrease in turbulent flow by an order of magnitude (compared to that of advection), Fig. 12. The effect on the advective flow is not as dominant, but a decrease in the amount of aerosols re-entrained into the canyon is observed. This is because the flux at that level is due to the upper circulatory vortex, driven by forced convection and of relatively lower concentration of aerosols. The lower vortex circulates the region of higher aerosol concentration.

At high buoyancy, windward wall heating leads to a change of flow regime and a consequent decrease in F_t to the same order of magnitude as F_a . At low values of Ri flux values were found to be relatively stable until a change of flow regime occurred, when flux values decreased by an order of magnitude, Figs. 13 and 14. This result is useful for developing parameterisations for windward heated walls. Future work on assessing the critical Richardson Number where this transition takes place at a range of flow conditions would be helpful in this regard.

These model results need to be validated with further field measurements since to date it is believed that numerical simulations overestimate buoyancy effects due to the fact that most full scale field measurements do not show a strong dependence of flow patterns on thermal effects (Solazzo, 2007; Louka, 2001; Oliveria-Panao, 2009), however, the measurements are few, difficult to conduct and not well aligned with model validation exercises. Nonetheless, the implications of a change in flow regime for the overall flux pattern would still be valid in spite of the current debate.

3.3.5 Mixed convection: heat flux

Finally, the influence of heat flux on aerosol flux from the street canyon was investigated. It is expected F_{Net} will increase with enhanced vertical heat flux due to the

Linking aerosol fluxes in street canyons to urban city-scale emissions

B. K. Tay et al.

Title Page

Abstract

Introduction

Conclusions

References

Tables

Figures



Back

Close

Full Screen / Esc

Printer-friendly Version

Interactive Discussion



increase in the vertical velocity arising from natural convection (buoyancy). However, flow within the canyon and the resultant flux is influenced by both forced convection and natural convection. Unless the flow regime is such that it is reinforced by an increase in buoyancy (e.g. leeward heated), the relationship between heat flux and net aerosol flux from the canyon would not be straight forward.

Local heat flux was estimated at the roof of the canyon and compared to the aerosol flux. Heat flux was calculated based on, $H_{\text{local}} = \int_L \left(-K_{\chi} \frac{\partial T}{\partial z} + T \bar{w} \right) dx$. Figures 15 and 16 show the relationship between heat and aerosol fluxes for the leeward and windward heated canyon walls, respectively as a function of U . For all cases, the net heat flux is negative which is expected as the steady state results show that the net effect of advection and turbulent diffusion is a containment of overall heat energy within the canyon, leading to an increase in the cavity temperature, whilst the above canyon temperature is not significantly affected by the heated walls within the canyon.

As shown in the leeward wall heated case, Fig. 15, the enhanced buoyancy due to increasing wall temperature reinforces the vortex. Therefore, the reduction in heat flux into the canyon due to increase in buoyancy is translated into enhanced aerosol flux. The sensitivity increases with reduction in forced convection. However, one notes that aerosol flux is a relatively weaker function of heat flux, H , compared to that with wind speed.

For the windward heated wall case, Fig. 16, it is observed that for $U=5$ m/s and 10 m/s, there is an increase in heat flux as aerosol flux decreases. The decrease is more pronounced at 2.5 m/s as it coincides with a change in flow regime. This simple exercise illustrates the fact that heat flux and aerosol flux within canyon scales do not necessarily correlate positively due to influences arising from both forced and natural convection and changes in flow regime, and the relationship as a result may be weak. This may explain why field observations within street canyons do not always show a clear enhancement of aerosol flux with local sensible heat flux. Above the urban canopy however the relationship may be different due to a transition to the usual mixed

Linking aerosol fluxes in street canyons to urban city-scale emissions

B. K. Tay et al.

Title Page

Abstract

Introduction

Conclusions

References

Tables

Figures



Back

Close

Full Screen / Esc

Printer-friendly Version

Interactive Discussion

boundary layer similarity scaling laws.

4 Limitations of the studies

These studies have only considered an infinitely long canyon, with the wind perpendicular to the canyon axis. They do not consider other wind directions or complex canyon geometry which may influence flux characteristics. Being 2-D in nature, the study does not consider the effects of lateral fluxes which will be significant. However, though limited in nature, it does provide valuable insights to the sensitivity of aerosol fluxes to a range of flow conditions. A further limitation is the use of the simplistic $k-\varepsilon$ turbulence model approach. When compared with Large Eddy Simulation (LES) models of street canyon dispersion, LES generally predicts a more uniform concentration distribution within the canyon, suggesting better turbulent mixing (Walton, 2002), i.e. there is an under-prediction of turbulent diffusion by the $k-\varepsilon$ model. Nonetheless, for these steady state results and for the purposes of these parametric studies, the method of turbulence closure is adequate providing insights into the governing micrometeorological factors to inform field measurement strategies.

5 Linking aerosol dispersion in urban canyons to cityscale emissions

Here we will attempt a first step towards reconciling tower micrometeorological aerosol flux measurements made above urban surfaces with the underlying source processes at the street canyon scale. The question that must be considered is whether micrometeorological tower flux measurements above cities can be useful in describing average behaviour of canyon aerosol sources and fluxes. There have been several field studies of city-scale aerosol emissions recently, Dorsey et al. (2002), Martensson et al. (2006) and Martin et al. (2008). These have attempted to investigate the relationship between F_{net} as a function of source parameters such as traffic activity, TA , and meteorological factors including wind speed, turbulence, atmospheric stability/and or sensible heat

Linking aerosol fluxes in street canyons to urban city-scale emissions

B. K. Tay et al.

Title Page

Abstract

Introduction

Conclusions

References

Tables

Figures

⏪

⏩

◀

▶

Back

Close

Full Screen / Esc

Printer-friendly Version

Interactive Discussion



Linking aerosol fluxes in street canyons to urban city-scale emissions

B. K. Tay et al.

Title Page

Abstract

Introduction

Conclusions

References

Tables

Figures

⏪

⏩

◀

▶

Back

Close

Full Screen / Esc

Printer-friendly Version

Interactive Discussion

flux. In most cases the studies found strong positive correlation between F_{net} and some of these factors (generally they show a weak dependence with traditional atmospheric stability parameters). Dorsey et al. (2002) proposed a parameterisation of the form $F_{\text{net}} = Ae^{1.6TA}$, where A is a constant, TA is the traffic activity (vehicles/s) and F_{net} is (#particles/cm²/s). They also derived a relationship between F_{net} in terms of the atmospheric stability parameter, $\zeta = -(z_m - d)/L$ (where z_m is the measurement height, d the urban canopy zero plane displacement and L the Monin-Obukov length which parameterises the buoyancy to shear driven scales of motion, and is given by $L = -\frac{u_*^3}{k\left(\frac{g}{T_0} \frac{H_0}{\rho C_p}\right)}$, see Monin and Obukov (1954), where T_0 and H_0 are the surface temperature and sensible heat fluxes, respectively, $k=0.4$, von Karman's constant, C_p is the specific heat capacity for air, g the acceleration due to gravity). However the parameterisation was only effective for moderate to strongly unstable cases. The study by Martensson et al. (2006) proposed a similar approach but used friction speed only; $F_{\text{Net}} = EF_{\text{fm}} TA \left(\frac{u_*}{\bar{u}_*}\right)^{0.4} + f_0$, where EF is an emission factor (vehicle/km – in their case they employed a mixed fleet emission factor), TA (in their case) is the traffic activity per unit area and time (vehicle km/m²/s), \bar{u}_* is the average friction velocity and f_0 is the contribution to UFP flux due to non-traffic related sources (and would be negative for losses by deposition). Martin et al. (2008) using data from the REPARTEE and CityFlux studies proposed that; $F_{\text{Net}} = D(a u_* + b H) + cTA + f_0$, where a , b and c are city specific emission factor constants related to friction speed, sensible heat flux and traffic activity, respectively, and D is a constant. TA , in their case, is the traffic activity (vehicles/s) measured at a random point or points within the flux footprint. The reported correlations with TA and u_* as expected were the strongest whilst that with sensible heat, H was the weakest.

It is naturally hypothesised that if above canyon micrometeorological aerosol flux measurements are taken above an extensive “uniform homogeneous network” of street canyons, then coupling exists between the measured flux footprint and the average flux expected at the street canyon top (“urban surface” emissions) in a simple manner. The

measured flux at the reference height is usually ascribed a micrometeorological “flux footprint” (e.g. Schuepp et al., 1990) encompassing a surface that conforms to the above definition so that the net flux measured is an aggregation of multiple canyon aerosol plumes e.g. Here we will compare the flux observations reported by Martin et al. (2008), with our simple canyon parameterisation model. In this approach we assume the following simplifications;

- The effects of horizontal advection and storage may be ignored;
- There is a well mixed region that dominates between the street canyon top-urban boundary layer transition zone and the measuring height;
- The aerosol transformation processes within the urban canopy layer will not influence the characteristics of the UFP aerosol number fluxes; and
- Sinks within the urban canopy have a minimal influence on the aerosol flux characteristics and can be ignored as a first approximation.

5.1 Results: aerosol emission fluxes

If these assumptions are valid then the measured and modelled fluxes will relate in a simple way through wind speed, turbulence and heat flux parameters at both scales. This similarity approach should reveal coupling of aerosol fluxes between both scales. For simplicity we have restricted the analysis to near isothermal cases. MATLAB[®] routines were used to fit the CFD results to the numerical model (Eq. 2.0), assuming u_* is directly proportional to Tl and that the contribution of advective flux may be neglected and therefore applicable in relating turbulent flux to wind and turbulence. A non-linear curve fitting was performed and the following numerical parameters recovered: $F_{\text{Net}} = \exp(9.92 + 1.12 \times 10^{-6} \ln U + 2.807l)$. Although this formulation was developed for near isothermal cases, it could be applied for unstable regimes, but, both modelling and observations suggest F_{Net} is a stronger function of wind speed or friction velocity,

Linking aerosol fluxes in street canyons to urban city-scale emissions

B. K. Tay et al.

Title Page

Abstract

Introduction

Conclusions

References

Tables

Figures

⏪

⏩

◀

▶

Back

Close

Full Screen / Esc

Printer-friendly Version

Interactive Discussion

compared to stability, (as is discussed below) at least for the city environments considered here so more work is required to refine this. When this is examined for relatively unstable conditions a positive correlation was found between the sensible heat flux and particle number flux, as reported by Martin et al. (2008), but correlation with local stability, ζ , was poor (also reported by Dorsey et al., 2002). In summary, if we compare a typical model prediction with an average diurnal observation of aerosol emission fluxes, using the REPARTEE and CityFlux datasets, the comparison yields a relatively poor correlation, $r^2=0.65$, with the model under-predicting fluxes at low wind speeds and over-predicting at higher wind speeds, Fig. 17.

This could be due to a number of reasons. The observational datasets used here were diurnal averages over a variety of different meteorological conditions and so may be biased in particular sectors for the city with respect to changes in source variability and surface morphology/TA activity affecting both the flux strength as well as the turbulence coupling regime. Heterogeneity in the source emission profiles comprising the average diurnal variations within the measurement footprints, and the lack of capture in detail of these source strengths, i.e. TA can explain some of the variability. In addition the complex interaction of natural convection and forced convection, especially within street canyon scales, which, unlike forced convection parameters such as wind and turbulent intensity, does not necessarily relate to an increase in aerosol flux. It also highlights the heterogeneity of urban surfaces involved (e.g. mixture of leeward, windward and ground heated street canyons) and the consequent variability in the effects of natural convection. More work should be undertaken to compare these CFD predictions to tower based flux data with greater canyon geometry and alignment footprint detail incorporated in the discussion in order to improve the results.

6 Summary

A systematic study was performed to assess the sensitivity of aerosol fluxes within and at roof level of idealized canyons to a range of canyon flow conditions. For all isother-

Linking aerosol fluxes in street canyons to urban city-scale emissions

B. K. Tay et al.

Title Page

Abstract

Introduction

Conclusions

References

Tables

Figures

⏪

⏩

◀

▶

Back

Close

Full Screen / Esc

Printer-friendly Version

Interactive Discussion



mal cases considered, turbulent flux dominates and is strongly related to wind speed (linear) and turbulent intensities (exponential). A parameterisation characterising this relationship was developed. As expected, for the case of windward and heated canyon walls this lead to a decrease in overall aerosol flux from canyons due to the opposing direction of buoyancy to the downward entrainment velocity at the windward side, whilst for the leeward heated wall case we observe a reinforcement of the existing vortex and this leads to an enhancement in the aerosol flux. Under high buoyancy conditions the effect of windward wall heating is to alter the flow regime and consequently decrease the turbulent aerosol flux component to the same order of magnitude as the aerosol advective flux, whilst the effect of leeward side heating is to increase the advective flux to the same order of magnitude as the turbulent aerosol flux.

Relative to U and TI , natural convection has a weaker influence on aerosol flux. Due to the complex interaction between both forced and natural convection, enhanced buoyancy does not necessarily lead to enhanced aerosol flux. When the flow regime is such that enhanced buoyancy would enhance any pre-existing vortex flow, such that overall flux increases as observed in the leeward heated case, a direct relation between the aerosol flux and Richardson number may be derived. Otherwise, such a direct relationship may not be possible, as shown in the windward heated case due to opposing effects of forced and natural convection. For the windward heated case, the aerosol flux was found to be fairly stable up to the point when the flow regime undergoes transition from a single to dual vortex flow regime.

A simple parameterization model for net canyon top aerosol emission fluxes was developed and may be applicable to future development of simple city-scale flux parameterisations, suggesting linkages between urban canopy dynamics and street canyon scales. Undoubtedly crude, these comparisons may be used as a starting point for linking mean street level concentrations (but not yet their variability) to those measured above the urban canopy roughness layer e.g. on micrometeorological towers. The relationship between aerosol flux and stability was found to be weak, possibly due to the complex interactions of mixed convective forces and heterogeneity of urban ge-

Linking aerosol fluxes in street canyons to urban city-scale emissions

B. K. Tay et al.

Title Page

Abstract

Introduction

Conclusions

References

Tables

Figures



Back

Close

Full Screen / Esc

Printer-friendly Version

Interactive Discussion

ometries. More work is needed to refine these linkage between CFD and tower based studies using improved statistical representations within flux footprint descriptions.

Acknowledgements. This work was supported by; DSO National Laboratories, Singapore. Data was provided by the NERC funded CityFlux grant, NE/B504865/1 and the REPARTEE project, funded by BOC Ltd.

References

- Baik, J. J. and Kim, J. J.: On the escape of pollutants from urban street canyons, *Atmos. Environ.*, 36, 527–536, 2002.
- Barlow, J. F. and Belcher, S. E.: A wind tunnel model for quantifying fluxes in the urban boundary layer, *Bound.-Lay. Meteorol.*, 104, 131–150, 2002.
- Belcher, S. E.: Mixing and transport in urban areas, *Philos. T. Roy. Soc. A.*, 363 (1837), 2947–2968, 2005.
- DePaul, F. T. and Sheih, C. M.: A tracer study of dispersion in an urban street canyon, *Atmos. Environ.*, 19, 555–559, 1985.
- DePaul, F. T. and Sheih, C. M.: Measurements of wind velocities in a street canyon, *Atmos. Environ.*, 20, 455–459, 1986.
- Dorsey, J. R., Nemitz, E., Gallagher, M. W., Fowler, D., Williams, P. I., Bower, K. N., and Beswick, K. M.: Direct measurements and parameterisation of aerosol flux, concentration and emission velocity above a city, *Atmos. Environ.*, 36, 791–800, 2002.
- Ferziger, J. H. and Peric, M.: *Computational Methods for Fluid Dynamics*, 3rd Edn., 423 pp., ISBN-3: 540-42074-6, Springer-Verlag, Berlin, Heidelberg, New York, 2001.
- Hunter, L. J., Johnson, G. T., and Watson, I. D.: An investigation of three dimensional characteristics of flow regimes within the urban canyon, *Atmos. Environ.*, 26B, 425–432, 1992.
- Johnson, J. T. and Hunter, L. J.: Some insights into typical urban canyon airflows, *Atmos. Environ.*, 33, 3991–3999, 1999.
- Ketzel, M., Louka, P., Sahn, P., Guilloteau, E., and Sini, J.-F.: Working group CFD modelling of the TRAPOS network: test case descriptions, preliminary results, <http://www2.dmu.dk/atmosphericenvironment/trapos/cfd-wg.htm>, 2000.
- Kumar, P., Garmory, A., Ketzel, M., Berkowicz, R., and Britter, R.: Comparative study of mea-

Linking aerosol fluxes in street canyons to urban city-scale emissions

B. K. Tay et al.

Title Page

Abstract

Introduction

Conclusions

References

Tables

Figures

⏪

⏩

◀

▶

Back

Close

Full Screen / Esc

Printer-friendly Version

Interactive Discussion

sured and modelled number concentrations of nanoparticles in an urban street canyon, *Atmos. Environ.*, 43, 949–958, 2009.

Longley, I.: High resolution measurements of turbulent transport of particulate matter in urban street canyons in Manchester, UK, PhD thesis, Dept. of Physics, UMIST, 317 pp., 2003.

5 Longley, I. D., Gallagher, M. W., Dorsey, J. R., and Flynn, M.: A case-study of fine particle concentrations and fluxes measured in a busy street canyon in Manchester, *Atmos. Environ.*, 38(22), 3595–3603, 2004.

Louka, P., Vachon, G., Sini, J. F., Mestayer, P. G., and Rosant, J. M.: Thermal effects on the airflow in a street canyon – Nantes’99 experimental results and model simulations, *Water Air Soil Pollut. Focus*, 2, 351–364, 2002.

10 Mårtensson, E. M., Nilsson, E. D., Buzorius, G., and Johansson, C.: Eddy covariance measurements and parameterisation of traffic related particle emissions in an urban environment, *Atmos. Chem. Phys.*, 6, 769–785, 2006,
<http://www.atmos-chem-phys.net/6/769/2006/>.

15 Martin, C., Longley, I. D., Dorsey, J. R., Thomas, R. M., Gallagher, M. W., and Nemitz, E.: Ultrafine particle fluxes above four major European cities, *Atmos. Environ.*, 44(1), 177–187, 2008.

Monin, A. S. and Obukov, A. M.: Basic laws of turbulent mixing in the ground layer of the atmosphere, *Acad. Nauk SSSR Tr. Geofiz. Inst.*, 245, 163–187, 1954.

20 Nakamura, Y. and Oke, T. R.: Wind, temperature and stability conditions in an east-west oriented urban canyon, *Atmos. Environ.*, 22, 2691–2700, 1988.

Oliveria Panoa, M. J. N., Gonclaves, H. J. P., and Ferrao, P. M. C.: Numerical analysis of the street canyon thermal conductance to improve urban design and climate, *Build. Environ.*, in press, 2009.

25 Patankar, S. V.: *Numerical Heat Transfer and Fluid Flow*, McGraw-Hill, New York, 197 pp., 1980.

Schuepp, P. H., Leclerc, M. Y., MacPherson, J. I., and Desjardins, R. L.: Footprint prediction of scalar fluxes, From analytical solutions of the diffusion equation, *Bound.-Lay. Meteorol.*, 50, 355–373, 1990.

30 Sini, J.-F., Anquetin, S., and Mestayer, P. G.: Pollutant dispersion and thermal effects in urban street canyon, *Atmos. Environ.*, 30 (15), 2659–2677, 1996.

Solazzo, E. and Britter, R. E.: Transfer processes in a simulated urban street canyon, *Bound.-Lay. Meteorol.*, 124, 43–60, 2007.

**Linking aerosol
fluxes in street
canyons to urban
city-scale emissions**

B. K. Tay et al.

Title Page

Abstract

Introduction

Conclusions

References

Tables

Figures

◀

▶

◀

▶

Back

Close

Full Screen / Esc

Printer-friendly Version

Interactive Discussion

Versteeg, H. K. and Malalasekera, W.: An Introduction to CFD. The Finite Volume Method, 2nd Edn., Longman, London, 2007.

Walton, A. and Cheng, A. Y. S.: Large-eddy simulation of pollution dispersion in an urban street canyon – Part II: idealised canyon simulation, Atmos. Environ., 36 (22), 3615–3627, 2002.

- 5 Whitby, E. R., McMurry, P. H., Shankar, U., and Binkowski, F. S.: Modal Aerosol Dynamics Modeling, Rep. 600/3-91/020, Atmospheric Research and Exposure Assessment Laboratory, US Environmental Protection Agency, Research Triangle Park, NC, available as NTIS PB911617291AS from National Technical Information Service, Springfield, VA, USA, 1991.

ACPD

9, 18065–18112, 2009

**Linking aerosol
fluxes in street
canyons to urban
city-scale emissions**

B. K. Tay et al.

Title Page

Abstract

Introduction

Conclusions

References

Tables

Figures

⏪

⏩

◀

▶

Back

Close

Full Screen / Esc

Printer-friendly Version

Interactive Discussion

Linking aerosol fluxes in street canyons to urban city-scale emissions

B. K. Tay et al.

Table 1. Aerosol size distributions assumed at the emission point.

	Aitken (UFP) mode	Accumulation mode
Number concentration (particles/m ³)	1×10^{11}	1×10^{10}
Geometric mean diameter (nm)	15	150
Standard deviation	1.5	1.6
Volume fraction (m ³ /m ³)	4.5×10^{-11}	

[Title Page](#)[Abstract](#)[Introduction](#)[Conclusions](#)[References](#)[Tables](#)[Figures](#)[I◀](#)[▶I](#)[◀](#)[▶](#)[Back](#)[Close](#)[Full Screen / Esc](#)[Printer-friendly Version](#)[Interactive Discussion](#)

Linking aerosol fluxes in street canyons to urban city-scale emissions

B. K. Tay et al.

Table 2. Model canyon and flow characteristics.

	Low	Medium	High
Aspect ratio (H/W)	0.50	1.0	2.00
Inflow turbulence intensity (TI) m^2/s^2	0.05	0.1	0.26
Inflow wind speed U (m/s)	2.50	5.0	10.00

[Title Page](#)[Abstract](#)[Introduction](#)[Conclusions](#)[References](#)[Tables](#)[Figures](#)[I◀](#)[▶I](#)[◀](#)[▶](#)[Back](#)[Close](#)[Full Screen / Esc](#)[Printer-friendly Version](#)[Interactive Discussion](#)

Linking aerosol fluxes in street canyons to urban city-scale emissions

B. K. Tay et al.

Table 3a. Leeward heated wall conditions.

Case	1	2	3	4	5	6	7	8
U (m/s)	10	10	10	5	5	5	5	5
ΔT (K)	4	10	15	2	4	6	10	15
Ri	0.0135	0.0338	0.0507	0.0271	0.0541	0.0812	0.1353	0.2030

[Title Page](#)[Abstract](#)[Introduction](#)[Conclusions](#)[References](#)[Tables](#)[Figures](#)[I◀](#)[▶I](#)[◀](#)[▶](#)[Back](#)[Close](#)[Full Screen / Esc](#)[Printer-friendly Version](#)[Interactive Discussion](#)

Linking aerosol fluxes in street canyons to urban city-scale emissions

B. K. Tay et al.

Table 3b. Leeward heated wall conditions.

Case	9	10	11	12	13
U (m/s)	2.5	2.5	2.5	2.5	2.5
ΔT (K)	4	6	8	10	15
Ri	0.217	0.325	0.433	0.541	0.812

[Title Page](#)[Abstract](#)[Introduction](#)[Conclusions](#)[References](#)[Tables](#)[Figures](#)[I◀](#)[▶I](#)[◀](#)[▶](#)[Back](#)[Close](#)[Full Screen / Esc](#)[Printer-friendly Version](#)[Interactive Discussion](#)

Linking aerosol fluxes in street canyons to urban city-scale emissions

B. K. Tay et al.

Table 3c. Windward heated wall.

Case	1	2	3	4	5	6	7	8	9
U (m/s)	10	10	10	5	5	5	2.5	2.5	2.5
ΔT (K)	4	10	15	4	10	15	4	10	15
Ri	0.0135	0.0338	0.0507	0.0541	0.1353	0.2030	0.2165	0.5412	0.8119

Title Page

Abstract

Introduction

Conclusions

References

Tables

Figures

I◀

▶I

◀

▶

Back

Close

Full Screen / Esc

Printer-friendly Version

Interactive Discussion

Linking aerosol fluxes in street canyons to urban city-scale emissions

B. K. Tay et al.

[Title Page](#)[Abstract](#)[Introduction](#)[Conclusions](#)[References](#)[Tables](#)[Figures](#)[I◀](#)[▶I](#)[◀](#)[▶](#)[Back](#)[Close](#)[Full Screen / Esc](#)[Printer-friendly Version](#)[Interactive Discussion](#)**Table 4.** Model fit parameters.

Aspect ratio	Coefficient values for proposed parameterisation		
	<i>a</i>	<i>b</i>	<i>c</i>
0.5	18.31	1.01	2.55
1	16.96	0.93	3.73
2	16.88	0.96	1.99

**Linking aerosol
fluxes in street
canyons to urban
city-scale emissions**

B. K. Tay et al.

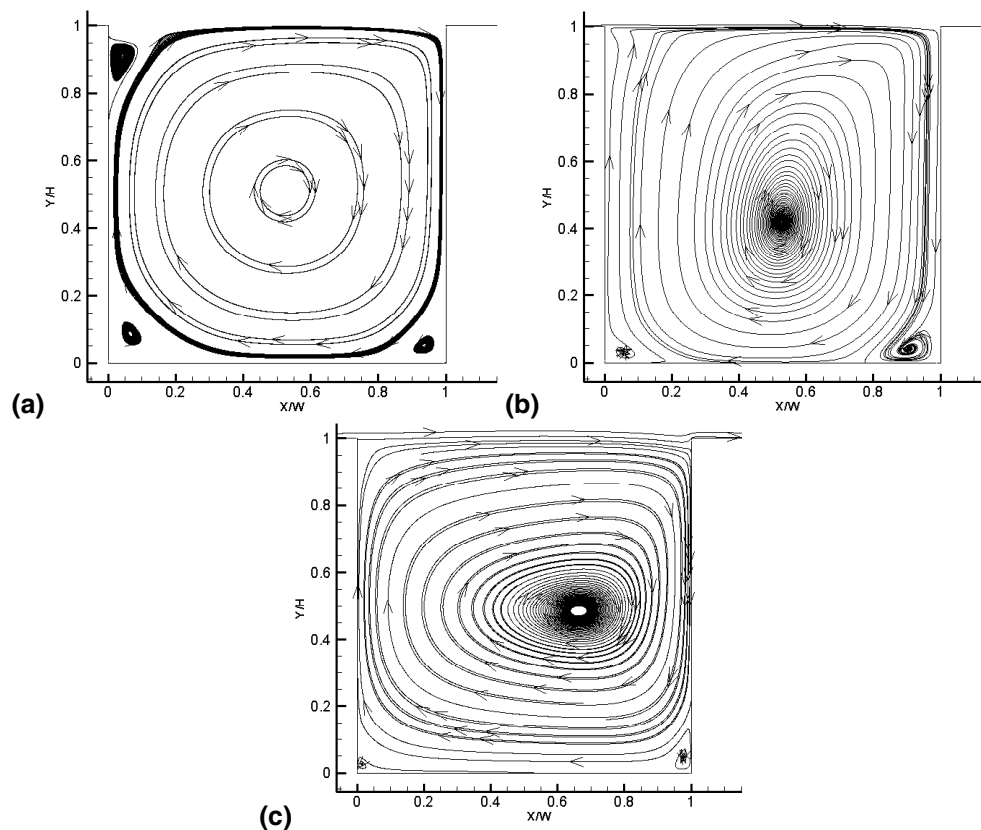


Fig. 1. Typical streamline patterns produced by the model for various canyon aspect ratios (AR): (a) $AR=1.0$; (b) $AR=2.0$ and (c) $AR=0.5$ (isothermal case with $U=5$ m/s and medium level turbulence). Vertical axis is normalised canyon height, horizontal axis is normalised by canyon width.

[Title Page](#)[Abstract](#)[Introduction](#)[Conclusions](#)[References](#)[Tables](#)[Figures](#)[◀](#)[▶](#)[◀](#)[▶](#)[Back](#)[Close](#)[Full Screen / Esc](#)[Printer-friendly Version](#)[Interactive Discussion](#)

Linking aerosol
fluxes in street
canyons to urban
city-scale emissions

B. K. Tay et al.

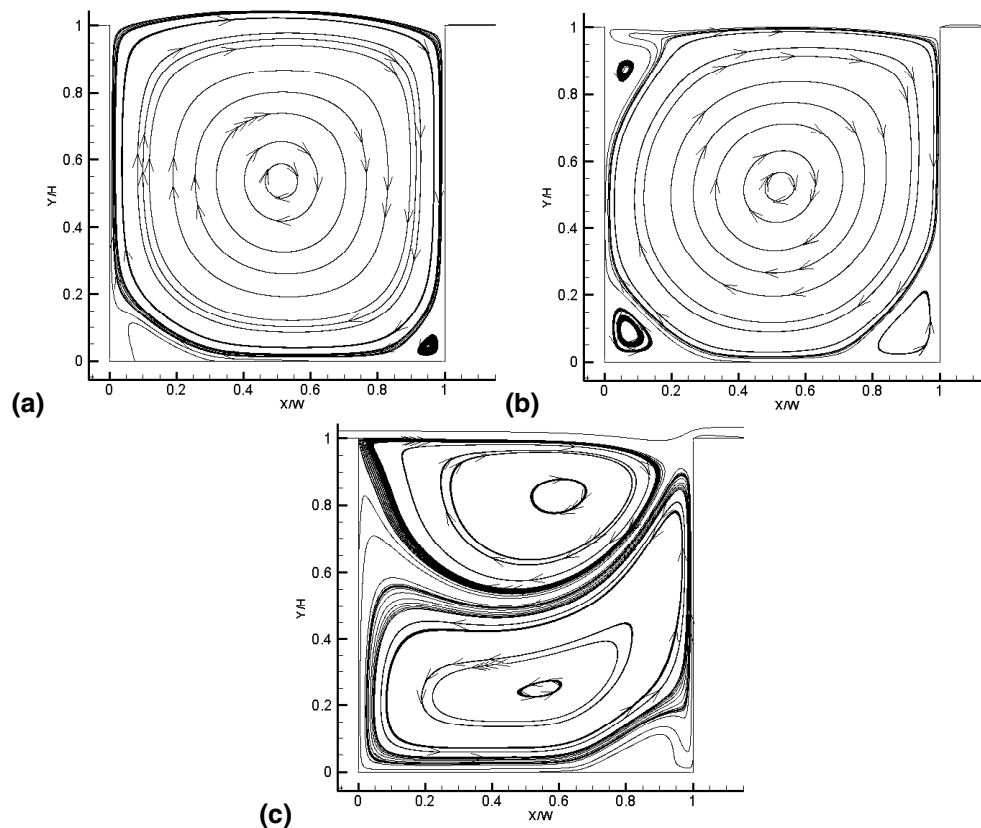


Fig. 2. Typical streamline patterns produced by model for (a): leeward heated wall ($U=2.5$ m/s, $\Delta T=15$ K); (b): for windward heated wall (mixed convection case for $s=2.5$ m/s, $\Delta T=4$ K) and (c): windward heated wall showing multiple vortices and transitional flow (for $U=2.5$ m/s, $\Delta T=15$ K). All cases for $AR=1.0$.

[Title Page](#)[Abstract](#)[Introduction](#)[Conclusions](#)[References](#)[Tables](#)[Figures](#)[◀](#)[▶](#)[◀](#)[▶](#)[Back](#)[Close](#)[Full Screen / Esc](#)[Printer-friendly Version](#)[Interactive Discussion](#)

Linking aerosol fluxes in street canyons to urban city-scale emissions

B. K. Tay et al.

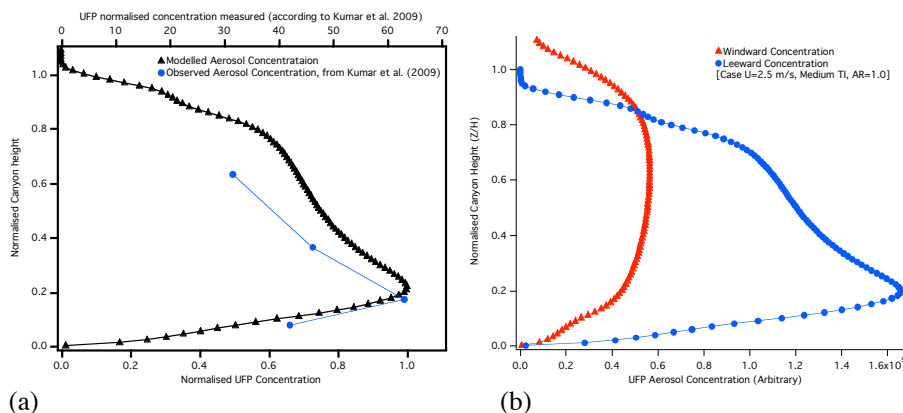


Fig. 3. (a) Example of leeward normalised UFP concentration profile as a function of normalised canyon height (Z/H), predicted by the model for low wind speeds ($U=2.5$ m/s) and medium turbulence intensities (see text), compared with field observations from Kumar et al. (2009); (b) Comparison of leeward and windward concentration profile for $U=2.5$ m/s, medium Tl and $AR=1.0$.

[Title Page](#)[Abstract](#)[Introduction](#)[Conclusions](#)[References](#)[Tables](#)[Figures](#)[◀](#)[▶](#)[◀](#)[▶](#)[Back](#)[Close](#)[Full Screen / Esc](#)[Printer-friendly Version](#)[Interactive Discussion](#)

Linking aerosol fluxes in street canyons to urban city-scale emissions

B. K. Tay et al.

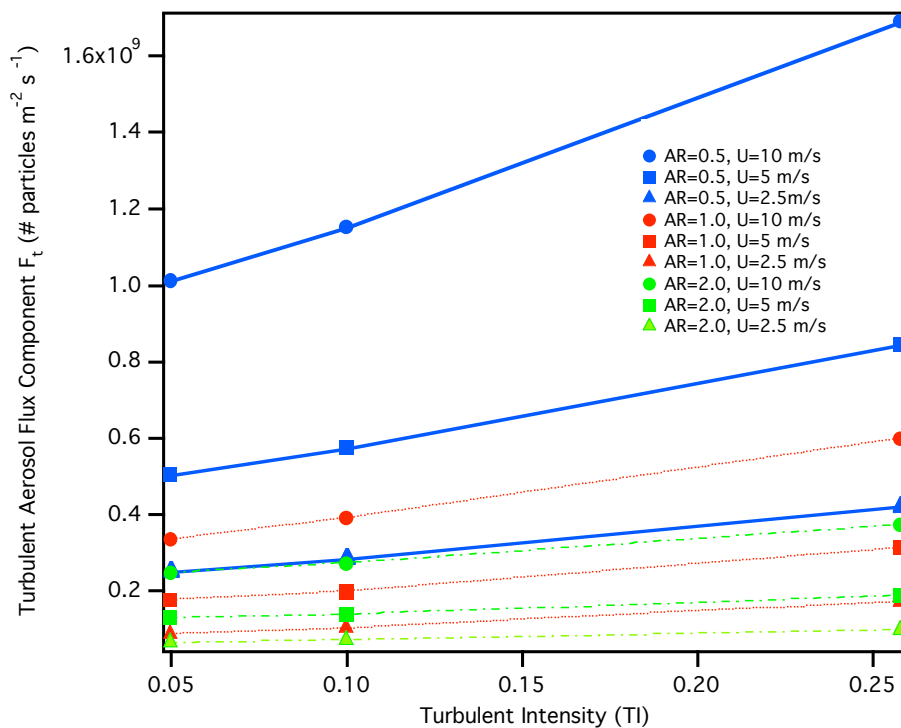


Fig. 4. Turbulent aerosol flux component, F_t ($\#$ particles m^{-2}/s) vs. turbulent intensity (TI) as a function of wind speed, U (m/s), and canyon aspect ratio $AR=0.5, 1.0$ and 2.0 .

Title Page

Abstract

Introduction

Conclusions

References

Tables

Figures

◀

▶

◀

▶

Back

Close

Full Screen / Esc

Printer-friendly Version

Interactive Discussion

Linking aerosol
fluxes in street
canyons to urban
city-scale emissions

B. K. Tay et al.

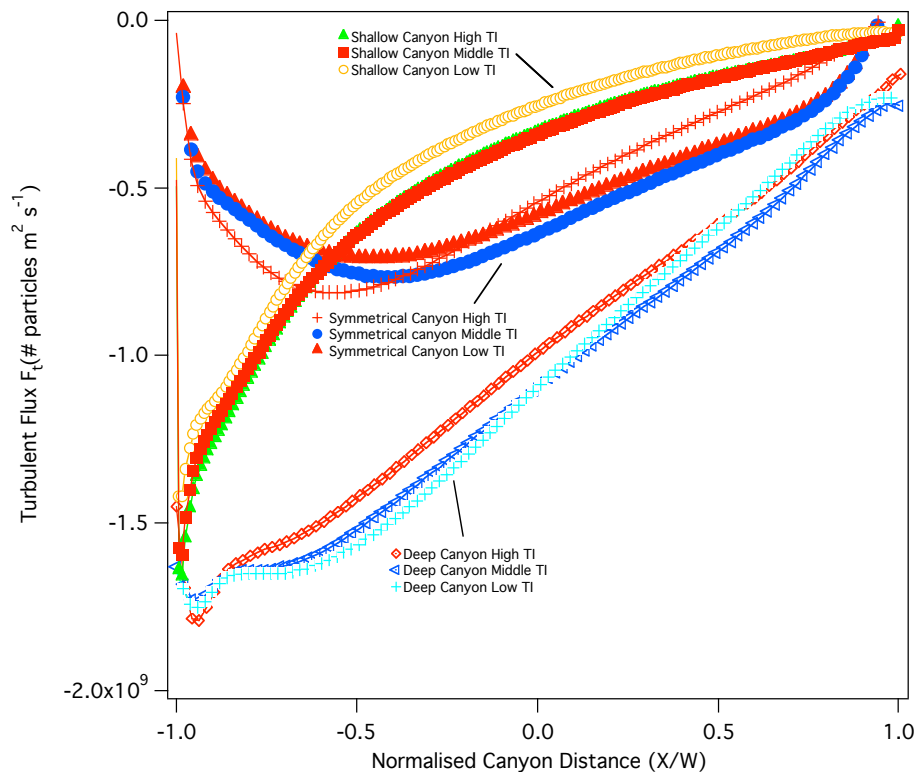


Fig. 5. Turbulent concentration shear profiles: Concentration shear profiles: d/dz vs. X/W , where X is the distance across the canyon and W is the canyon width for shallow ($H < W$), square ($H = W$) and deep ($H > W$) canyon aspect ratios, and for low, medium and high turbulence intensities (TI) (see text).

[Title Page](#)[Abstract](#)[Introduction](#)[Conclusions](#)[References](#)[Tables](#)[Figures](#)[I◀](#)[▶I](#)[◀](#)[▶](#)[Back](#)[Close](#)[Full Screen / Esc](#)[Printer-friendly Version](#)[Interactive Discussion](#)

Linking aerosol fluxes in street canyons to urban city-scale emissions

B. K. Tay et al.

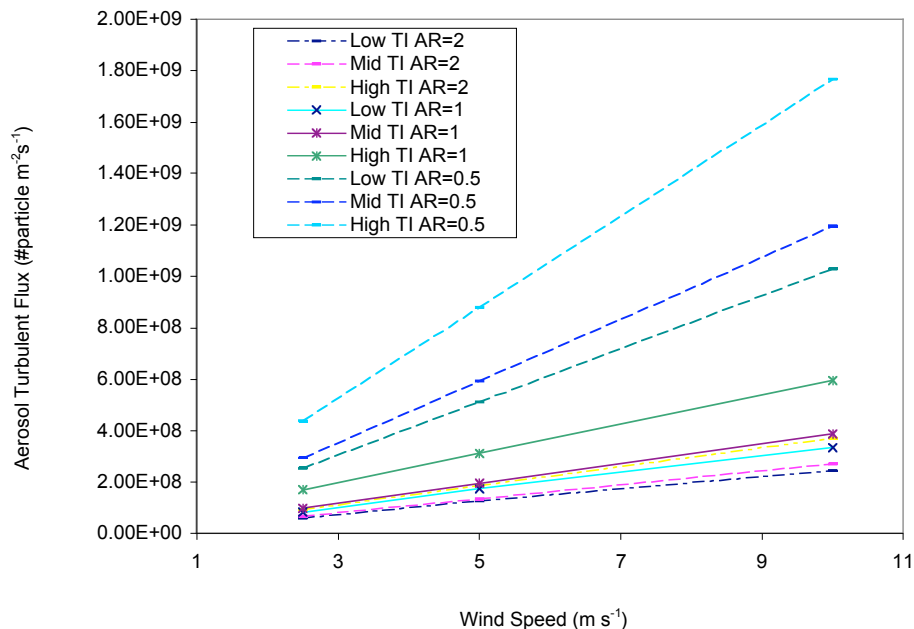


Fig. 6. Turbulent aerosol flux component, F_t , vs. wind speed, U (m/s), for low, medium and high turbulent intensity cases, TI , and canyon aspect ratios $AR=0.5, 1.0$ and 2.0 .

Title Page

Abstract

Introduction

Conclusions

References

Tables

Figures

◀

▶

◀

▶

Back

Close

Full Screen / Esc

Printer-friendly Version

Interactive Discussion

Linking aerosol fluxes in street canyons to urban city-scale emissions

B. K. Tay et al.

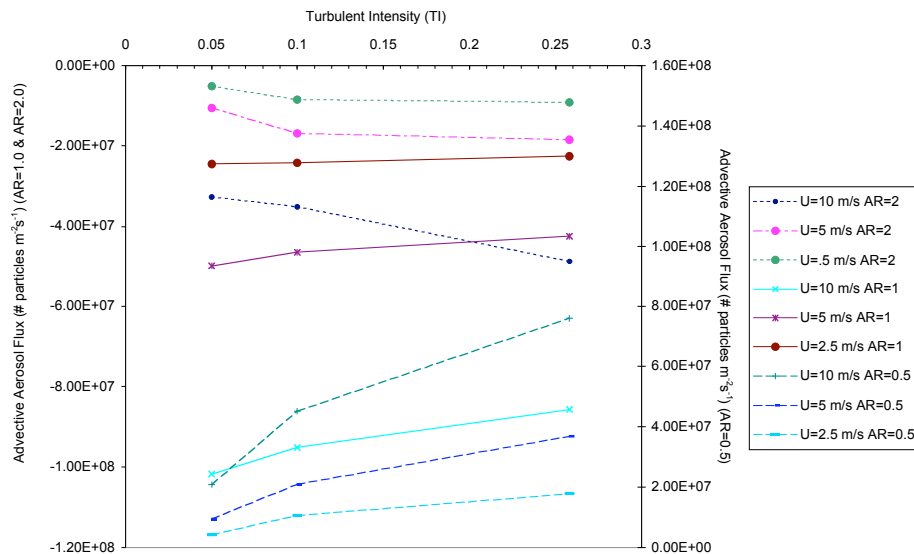


Fig. 7. Net aerosol flux, F_{Net} , vs. turbulent intensity, TI , as a function of wind speed $U=2.5, 5$ and 10 m/s and canyon aspect ratios $AR=0.5, 1.0$ and 2.0 .

Title Page

Abstract

Introduction

Conclusions

References

Tables

Figures

◀

▶

◀

▶

Back

Close

Full Screen / Esc

Printer-friendly Version

Interactive Discussion

Linking aerosol fluxes in street canyons to urban city-scale emissions

B. K. Tay et al.

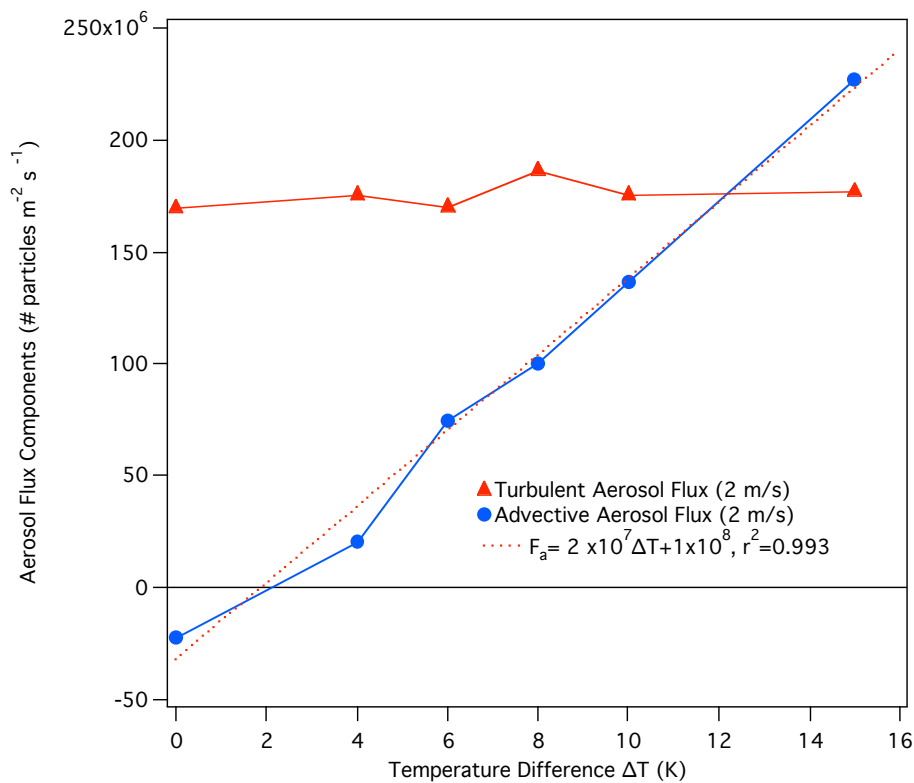


Fig. 8. Aerosol flux components (F_t and F_a) vs. wall temperature difference ΔT (K) for $U=2.5$ m/s.

[Title Page](#)[Abstract](#)[Introduction](#)[Conclusions](#)[References](#)[Tables](#)[Figures](#)[◀](#)[▶](#)[◀](#)[▶](#)[Back](#)[Close](#)[Full Screen / Esc](#)[Printer-friendly Version](#)[Interactive Discussion](#)

Linking aerosol fluxes in street canyons to urban city-scale emissions

B. K. Tay et al.

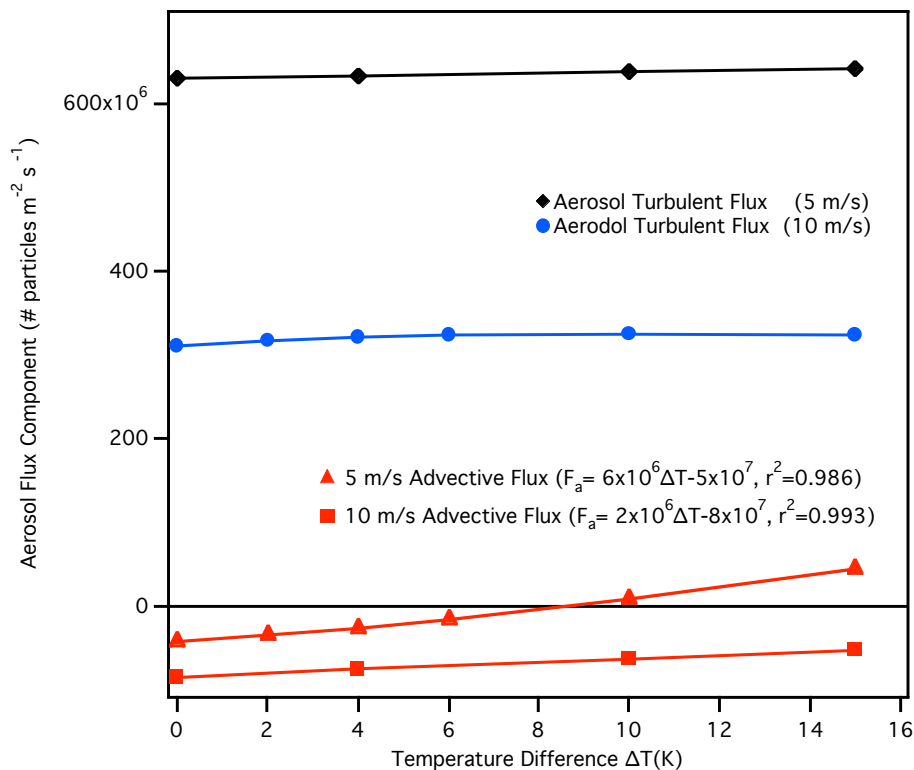
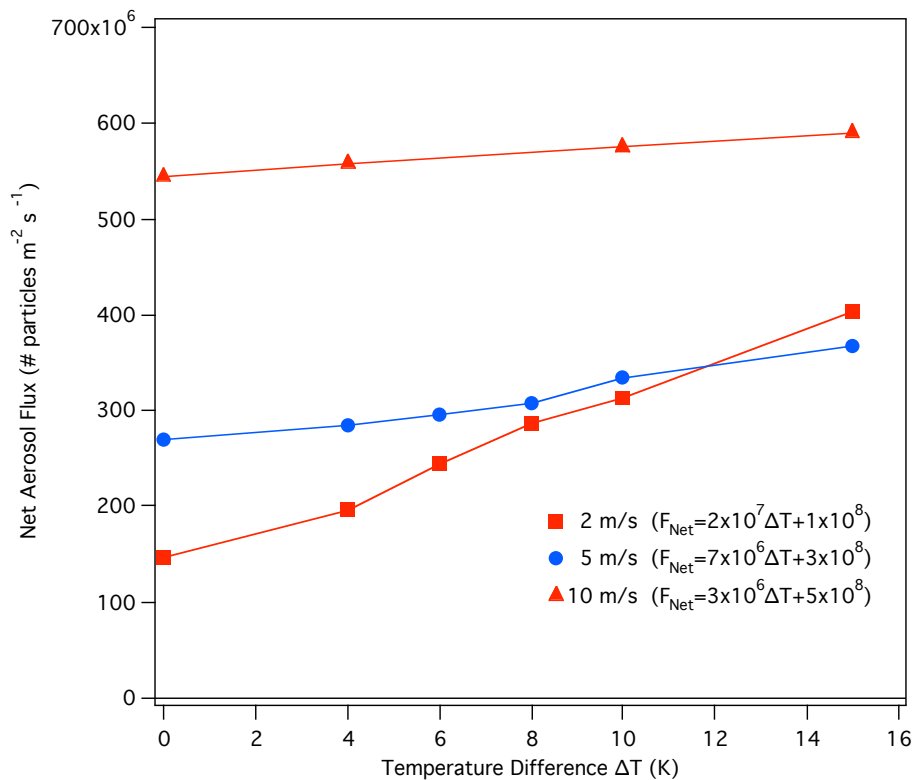


Fig. 9. Aerosol flux components (F_t and F_a) vs. wall temperature difference ΔT (K), for $U=5$ m/s and 10 m/s. Regression analyses are for F_a for $U=5$ and 10 m/s cases.

[Title Page](#)[Abstract](#)[Introduction](#)[Conclusions](#)[References](#)[Tables](#)[Figures](#)[⏪](#)[⏩](#)[◀](#)[▶](#)[Back](#)[Close](#)[Full Screen / Esc](#)[Printer-friendly Version](#)[Interactive Discussion](#)

Linking aerosol fluxes in street canyons to urban city-scale emissions

B. K. Tay et al.

**Fig. 10.** Net aerosol flux, F_{Net} , vs. temperature difference, ΔT (K).

Title Page

Abstract

Introduction

Conclusions

References

Tables

Figures

◀

▶

◀

▶

Back

Close

Full Screen / Esc

Printer-friendly Version

Interactive Discussion

Linking aerosol fluxes in street canyons to urban city-scale emissions

B. K. Tay et al.

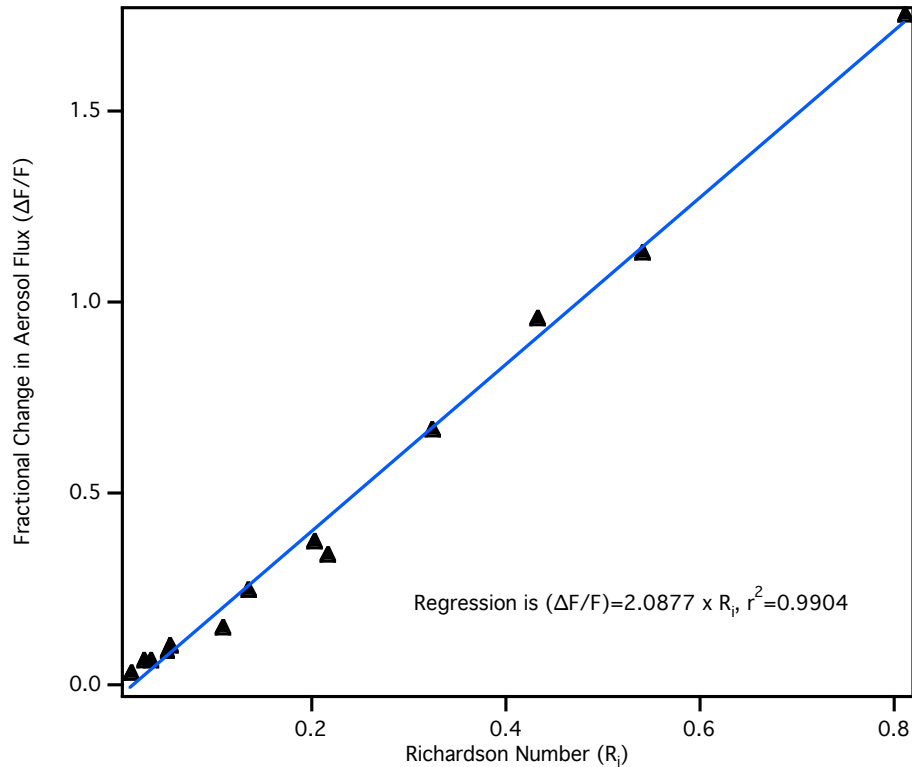


Fig. 11. Enhancement of aerosol flux ($\Delta F/F$) vs. Richardson number, R_i , for the leeward heated wall case.

[Title Page](#)[Abstract](#)[Introduction](#)[Conclusions](#)[References](#)[Tables](#)[Figures](#)[⏪](#)[⏩](#)[◀](#)[▶](#)[Back](#)[Close](#)[Full Screen / Esc](#)[Printer-friendly Version](#)[Interactive Discussion](#)

Linking aerosol fluxes in street canyons to urban city-scale emissions

B. K. Tay et al.

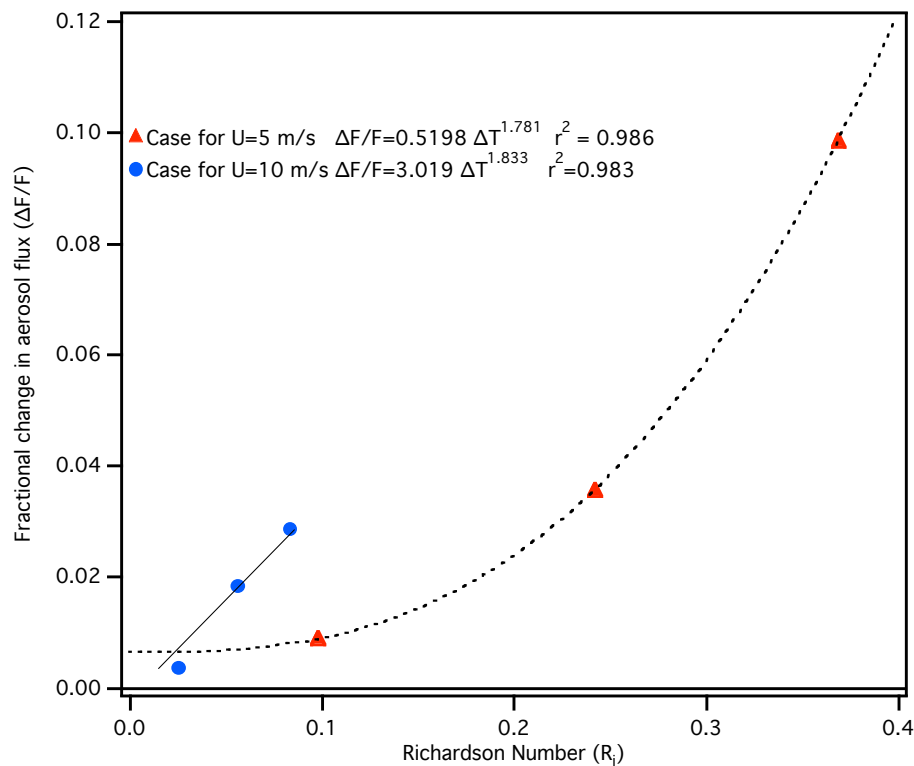


Fig. 12. Fractional change in net aerosol flux, $\Delta F/F$, vs. Richardson number, R_i , for the windward heated wall case and for $U=5$ m/s and 10 m/s.

[Title Page](#)[Abstract](#)[Introduction](#)[Conclusions](#)[References](#)[Tables](#)[Figures](#)[◀](#)[▶](#)[◀](#)[▶](#)[Back](#)[Close](#)[Full Screen / Esc](#)[Printer-friendly Version](#)[Interactive Discussion](#)

Linking aerosol fluxes in street canyons to urban city-scale emissions

B. K. Tay et al.

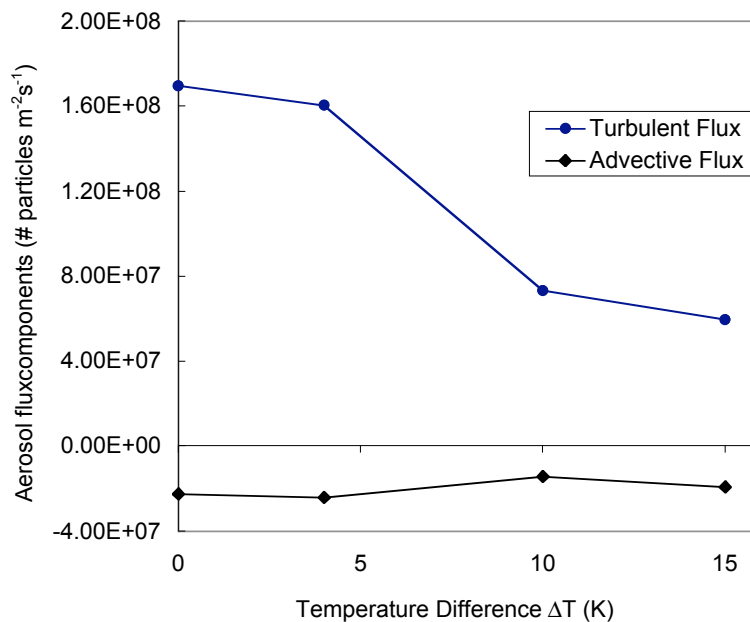


Fig. 13. Aerosol flux components, F_t and F_a vs. wall temperature for $U=2.5$ m/s.

[Title Page](#)[Abstract](#)[Introduction](#)[Conclusions](#)[References](#)[Tables](#)[Figures](#)[◀](#)[▶](#)[◀](#)[▶](#)[Back](#)[Close](#)[Full Screen / Esc](#)[Printer-friendly Version](#)[Interactive Discussion](#)

Linking aerosol fluxes in street canyons to urban city-scale emissions

B. K. Tay et al.

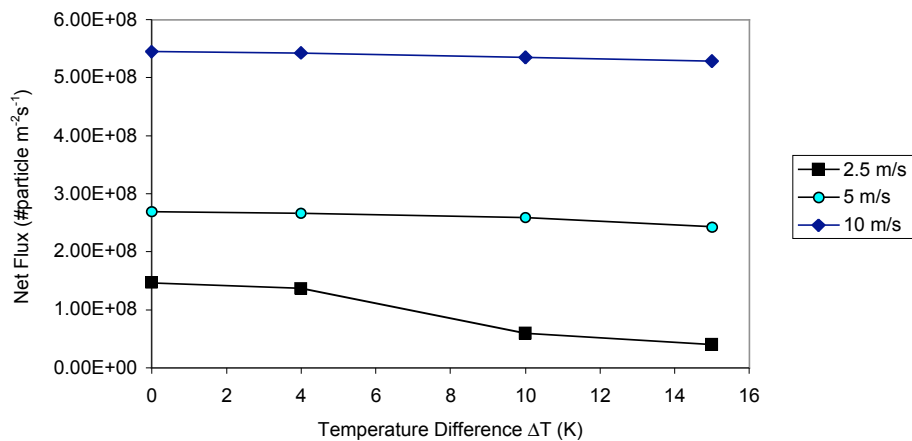


Fig. 14. Net aerosol flux, F_{Net} , vs. temperature difference, ΔT (K), for $U=2.5, 5.0$ and 10.0 m/s.

[Title Page](#)[Abstract](#)[Introduction](#)[Conclusions](#)[References](#)[Tables](#)[Figures](#)[⏪](#)[⏩](#)[◀](#)[▶](#)[Back](#)[Close](#)[Full Screen / Esc](#)[Printer-friendly Version](#)[Interactive Discussion](#)

Linking aerosol fluxes in street canyons to urban city-scale emissions

B. K. Tay et al.

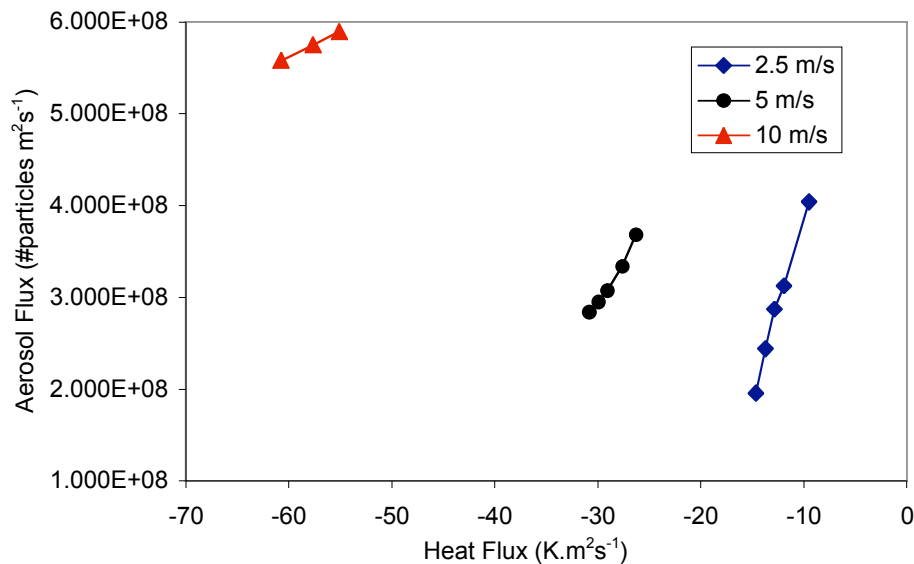


Fig. 15. Net aerosol flux, F_{Net} , vs. canyon top local heat flux, H , ($\text{K}\cdot\text{m}^2\cdot\text{s}^{-1}$) for the leeward heated wall case and for $U=2.5$, 5.0 and 10.0 m/s.

[Title Page](#)[Abstract](#)[Introduction](#)[Conclusions](#)[References](#)[Tables](#)[Figures](#)[◀](#)[▶](#)[◀](#)[▶](#)[Back](#)[Close](#)[Full Screen / Esc](#)[Printer-friendly Version](#)[Interactive Discussion](#)

Linking aerosol fluxes in street canyons to urban city-scale emissions

B. K. Tay et al.

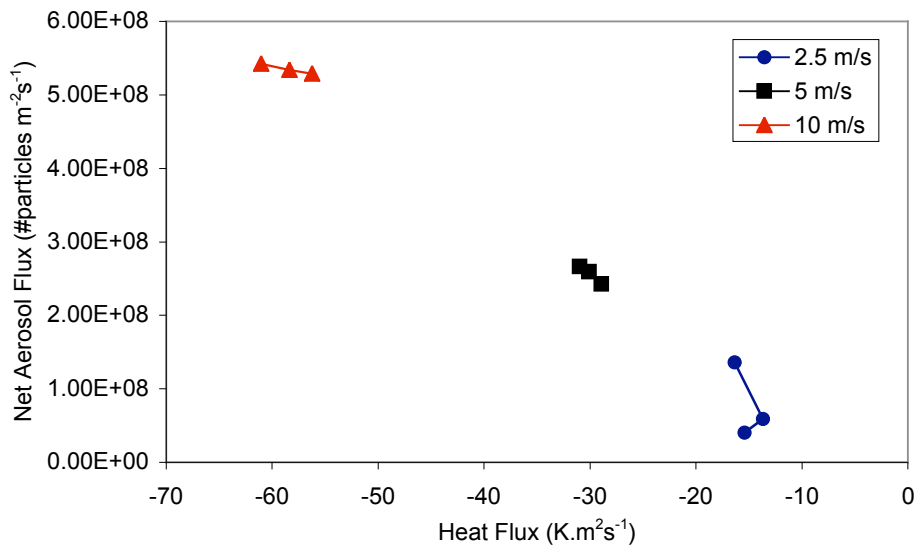


Fig. 16. Aerosol flux, F_{Net} , versus canyon top local heat flux, H , ($\text{K m}^{-2} \text{s}^{-1}$) for the windward heated wall case and for $U=2.5, 5.0$ and 10.0 m/s.

[Title Page](#)[Abstract](#)[Introduction](#)[Conclusions](#)[References](#)[Tables](#)[Figures](#)[⏪](#)[⏩](#)[◀](#)[▶](#)[Back](#)[Close](#)[Full Screen / Esc](#)[Printer-friendly Version](#)[Interactive Discussion](#)

Linking aerosol fluxes in street canyons to urban city-scale emissions

B. K. Tay et al.

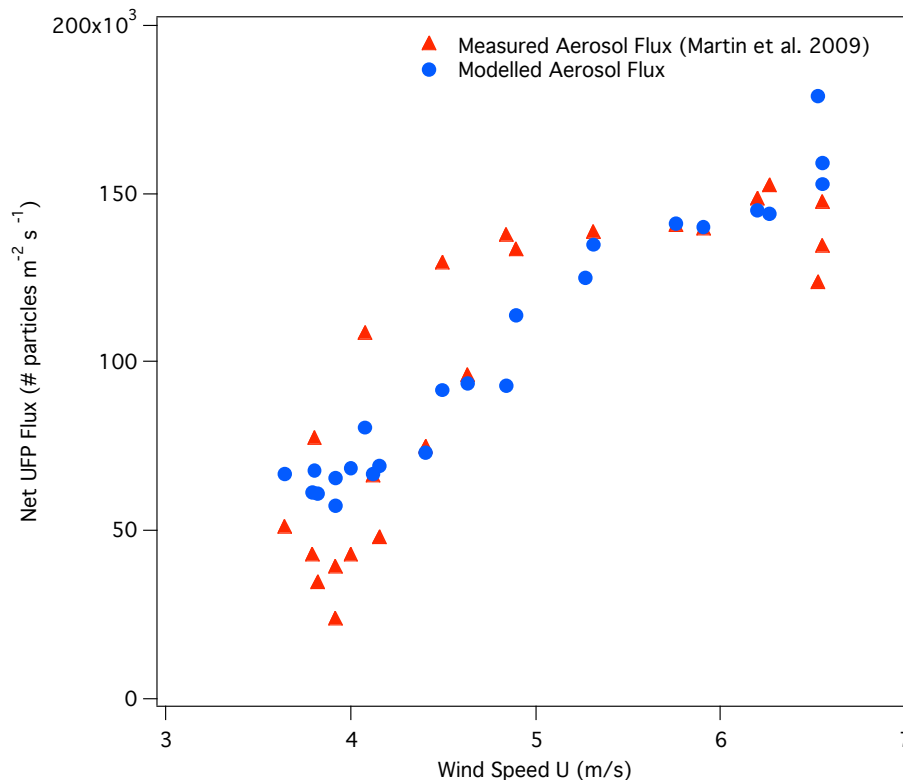


Fig. 17. Modelled UFP aerosol flux compared with observed UFP average diurnal aerosol flux range (REPARTEE/CityFlux data from Martin et al., 2008), ($r^2=0.65$).

Title Page

Abstract

Introduction

Conclusions

References

Tables

Figures

◀

▶

◀

▶

Back

Close

Full Screen / Esc

Printer-friendly Version

Interactive Discussion